Mixed conduction and oxygen permeation in the substituted oxides for CaTiO$_3$

H. IWAHARA, T. ESAKA, T. MANGAHARA

Department of Environmental Chemistry and Technology, Faculty of Engineering, Tottori University, Minami 4-101, Koyama-cho, Tottori 680, Japan
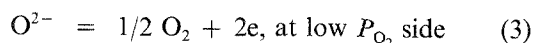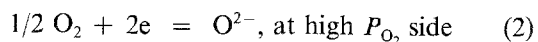
Mixed conduction in substituted perovskite-type oxides CaTi$_{1-x}$M$_x$O$_{3-\alpha}$ (M = Fe, Co and Ni) was studied by means of electrochemical methods. Of these materials, Fe-substituted oxides showed the highest oxide ion conductivity as well as high electronic conductivity. The oxide ion transport numbers of the oxides were lower than 0.6 over the whole composition range measured in air. Electrochemical oxygen permeation in such a material could be confirmed by gas chromatography. Extraction of oxygen from air was carried out using the mixed conductor. The oxygen extraction rate in this method was higher than that using a silicone film.

1. Introduction

A mixed conductor in which both oxide ions and electrons are mobile has potential use for separation of pure oxygen from air or other oxygen containing gases since the oxygen can permeate electrochemically through such a material in the form of oxide ions. The principles of oxygen gas extraction from air using a pure oxide ion conductor and a mixed conductor are schematically illustrated in Fig. 1. In the former case (a), when one side of the conductor diaphragm is exposed in air and another side is evacuated by vacuum pump, an electrochemical oxygen gas concentration cell is formed and the electromotive force, E_0, is generated according to the difference in oxygen partial pressures between the both sides of the cell,

$$E_0 = (RT/4F) \ln [0.21/P_{O_2}, 1] \qquad (1)$$

where R, T and F have their usual meanings and P_{O_2}, 1 is the oxygen partial pressure in the evacuated side. If the porous electrode materials (e.g. porous platinum) are attached to both sides of the ionic conductor and they are short-circuited, the oxide ions in the conductor migrate toward the electrode of low partial pressure of oxygen (anode), and the cell is discharged according to the following electrode reactions.

$$1/2 \, O_2 + 2e = O^{2-}, \text{ at high } P_{O_2} \text{ side} \qquad (2)$$

$$O^{2-} = 1/2 \, O_2 + 2e, \text{ at low } P_{O_2} \text{ side} \qquad (3)$$

As a result, oxygen gas is generated at the anode and thus pure oxygen can be extracted electrochemically.

In the latter case however, (b) in Fig. 1, only evacuation would be enough to extract the oxygen, and both electrode and connecting lead are unnecessary, as the cell is short-circuited by electronic conduction in the mixed conductor.

Previously, we reported several kinds of mixed conductors based on Bi$_2$O$_3$ [1, 2], ZrO$_2$ [3] and CaTiO$_3$ [4]. In the last case, the sintered oxides of CaTi$_{1-x}$Al$_x$O$_{3-\alpha}$

are oxide ionic and electronic mixed conductors and the oxide ion conductivities are almost comparable to those of calcia-stabilized zirconias. But the total conductivity was not enough for the use of oxygen extraction. In the present study, some transition metals were substituted for the Ti sites of CaTiO$_3$ in order to improve ionic and electronic conduction. We report here the mixed conduction in the transition metal-substituted CaTiO$_3$ and the result of oxygen extraction experiment using these materials.

2. Experimental details

2.1. Preparation of samples

The samples were prepared from reagent grade powders of oxides or carbonates of the corresponding metals. These materials were weighed in the defined molar ratios, mixed in an agate mortar, and fired at 1100°–1400° C in air for 10 h. The fired oxides were ground, pressed hydrostatically (2 t cm^{-2}) into column-shaped (4–5 mm diameter by 7–10 mm length) and disk-shaped samples (10–12 mm diameter by 1–2 mm thickness), and sintered again under the same condition as the first firing. X-ray diffraction was carried out using CuKα-radiation to identify the crystal phase of the prepared samples.

2.2. Measurement of ionic conductivity

The electrical conductivity of specimens was measured using an AC bridge with a 10 kHz signal. Column-shaped specimens were generally employed in this measurement. Platinum powder paste was smeared on both ends of the samples, and fired to serve as the electrode. The ionic transport number of specimens was determined from the e.m.f. of an oxygen gas concentration cell constructed using a disk specimen as an electrolyte. 1 atm air and oxygen were used as the anode and cathode gas, respectively.
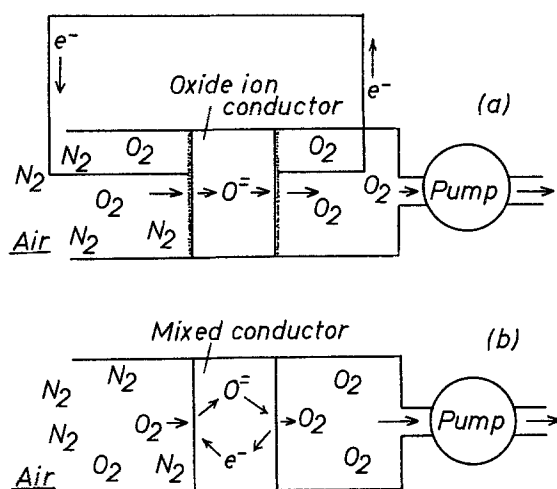
Fig. 1. Schematic diagram of oxygen extraction from the air using (a) an oxide ion conductor and (b) a mixed conductor.

2.3. Oxygen permeation

Oxygen permeation experiment was carried out by detecting the oxygen gas generated at the lower pressure side. The sample used here is a one end-closed ceramic tube (interior surface area: about $15\,cm^2$, thickness: about 1 mm). As indicated in Fig. 2, the sample was held between two ceramic tubes via a glass packing. After fusion of the packing at high temperature, the outside of sample was exposed to air and the inside was evacuated by diaphragm vacuum pump. The gas obtained in the lower pressure side was kept in the container B (Fig. 2). After putting the atmosphere back to the normal pressure, the gas volume and the purity were checked. The gas chromatograph was used to analyse the oxygen content of the extracted gas. In a special case, the gas was directly sampled from the outlet of the diaphragm pump without usage of the containers A and B.
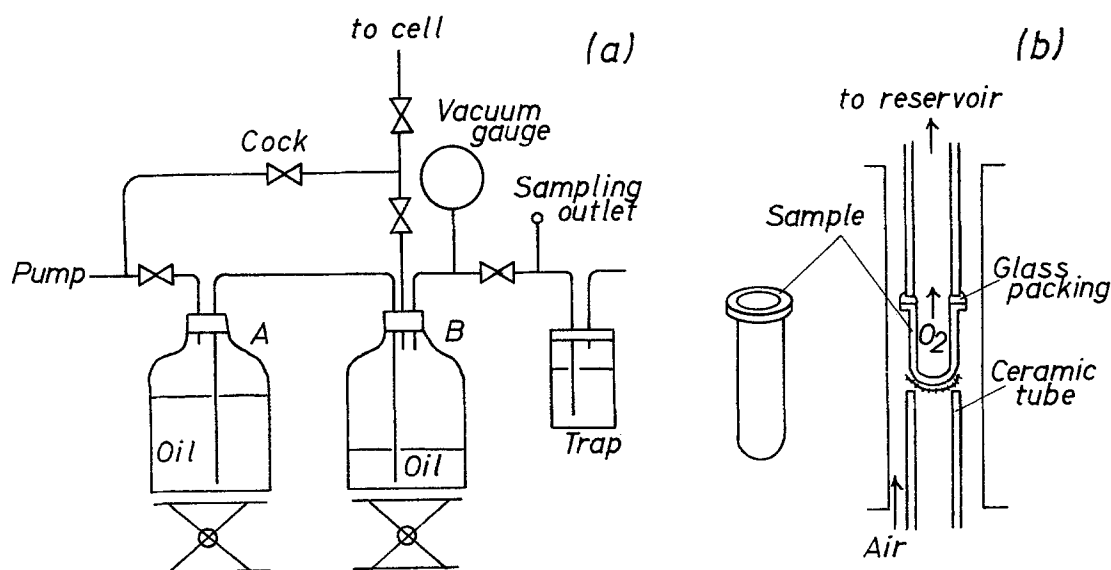
3. Results and discussion

3.1. Crystal phase

Fig. 3 shows X-ray diffraction patterns of the typical specimens in the system $CaTi_{1-x}Fe_xO_{3-\alpha}$, $x = 0.0-0.6$. The specimens of $x = 0.0-0.25$ show patterns of the pseudo-cubic phase which corresponds to one of the JCPDS card data of $CaTiO_3$. The crystal phase in the samples $x = 0.3-0.5$ was cubic. The specimen of $x = 0.6$ shows a mixed phase with the perovskite-type cubic and the unknown.

Besides iron, we tried cobalt and nickel as substituents for the titanium site in $CaTiO_3$. The solid solution formation range, however, was limited to $x = 0.1$ or less and the cubic phase was not present in the higher content range of the substituents.

3.2. Conductivity

The unsubstituted $CaTiO_3$ showed low conductivities. Although conductivity could not be markedly improved in the case of nickel substitution, iron substitution caused a clear conductivity increase. Fig. 4 indicates Arrhenius plots of the conductivity of $CaTi_{1-x}Fe_xO_{3-\alpha}$ for the representative compositions. The conductivities increase with increasing content of the substituents. In the system $CaTi_{1-x}Co_xO_{3-\alpha}$, the conductivity was also enhanced by cobalt substitution. However, the samples of $x > 0.2$ having high conductivities showed a mixed phase with $CaTiO_3$ and another. Therefore we will only mention below the results for the samples in the system $CaTi_{1-x}Fe_xO_{3-\alpha}$.

3.3. Conduction properties

The oxygen concentration cells using these specimen disks as electrolytes showed some electromotive forces
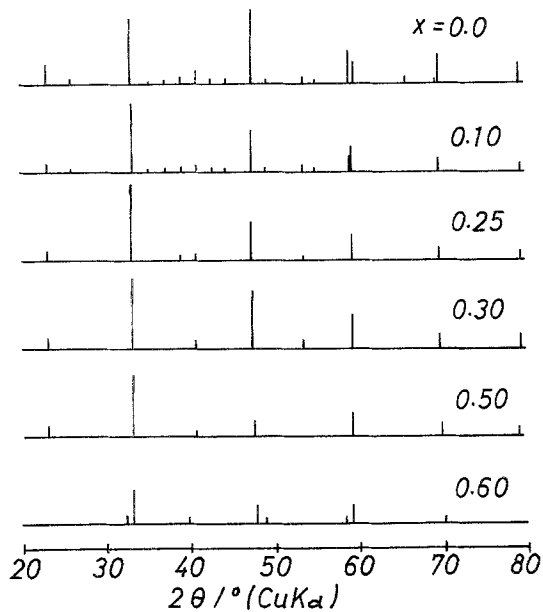

Fig. 2. Schematic diagram of the oxygen extracting apparatus. (a) Gas reservoir, (b) cell construction.

Fig. 3. X-ray diffraction patterns of CaTi$_{1-x}$Fe$_x$O$_{3-x}$.

Fig. 5. Transport number of oxide ion measured by an oxygen concentration cell. Specimen: CaTi$_{1-x}$Fe$_x$O$_{3-x}$.

(E). These were compared with the theoretical values (E_0) calculated by the Nernst equation. Fig. 5 shows the E/E_0 values versus temperature relationships for various samples. The ratio is the highest in the specimen of $x = 0.2$ and it increases with increasing temperature. However, the values were substantially lower than unity indicating that electrons as well as ions take part in the conduction process simultaneously.

When the concentration cells were discharged, steady and stable currents could be drawn and the sample resistances calculated from the current vs voltage relations were almost the same as those measured by AC bridge. These results indicate that the mobile ions in the conductor are oxide ions since the electrode reactions (2) and (3) can proceed reversibly in that case.

When electronic conductivity is higher than oxide ion conductivity, E/E_0 values often given incorrect transport number because of polarization at the electrode. The ionic transport numbers of E/E_0 were com-
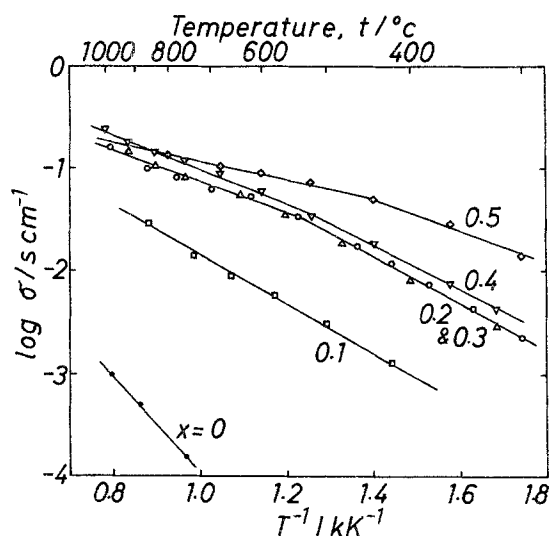
pared with those of $1 - I_e/G_tE_0$, which were calculated from total conductance (G_t) and electronic current (I_e) measured by applying the theoretical voltage (E_0) of the concentration cell to stop the ionic current [5]. These data were almost the same as those of E/E_0.

In order to check the electronic charge carriers (electrons or electron holes) in the samples, the conductivities were measured in the various oxygen atmospheres for the representative samples ($x = 0.2$ and 0.4). In both cases, the conductivities decreased with decreasing oxygen partial pressure. This suggests that electronic conduction due to electron holes takes place in these specimens. If the irons in the oxide are trivalent, oxide ion vacancies □ are formed stoichiometrically according to the following equation,

$$CaO + (1 - x)TiO_2 + (x/2)Fe_2O_3$$

$$= CaTi_{1-x}Fe_xO_{3-0.5x}□_{0.5x}, \quad (4)$$
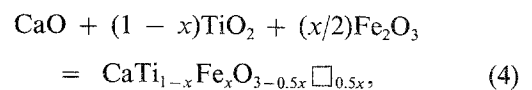
and electronic conduction could not be observed. However, as the irons in the perovskite-type oxides

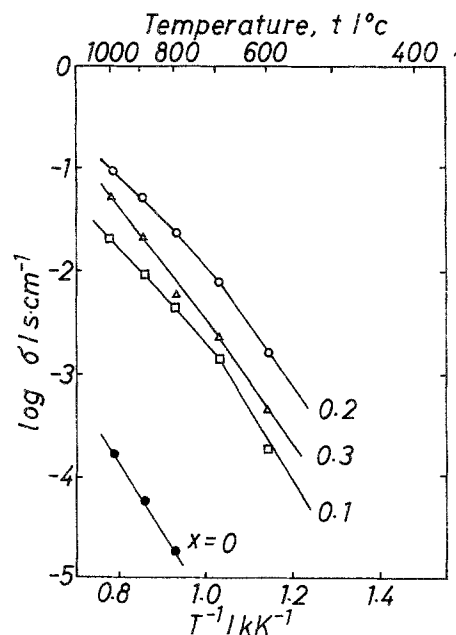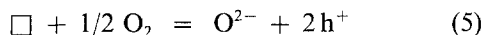Fig. 4. Arrhenius plots of the total conductivity of CaTi$_{1-x}$Fe$_x$O$_{3-x}$ measured in air.

Fig. 6. Arrhenius plots of ionic conductivity of CaTi$_{1-x}$Fe$_x$O$_{3-x}$.

can change their valence to higher states than trivalent, the accompanying oxygen can occupy the oxide ion vacancies as follows,

$$\square + 1/2\,O_2 = O^{2-} + 2\,h^+ \tag{5}$$

and hole conduction will appear.

The results of conductivity and ionic transport number measurements show that some samples in the system $CaTi_{1-x}Fe_xO_{3-\alpha}$ have high oxide ion conductivity together with high electronic conductivity. Arrhenius plots of ionic conductivity of the typical samples are shown in Fig. 6. These values were obtained from the results of total conductivity and ionic transport number measurements mentioned above. While σ_e increases with increasing content of iron (Fig. 4), σ_i shows maximum values at $x = 0.2$. The conductivity $9.8 \times 10^{-2}\,S\,cm^{-1}$ at $1000°C$ is several times higher than CSZ and the activation energy $0.94\,eV$ is almost the same as that of CSZ.

3.4. Oxygen permeation

Using $CaTi_{0.8}Fe_{0.2}O_{3-\alpha}$, which shows the highest oxide ion conductivity and the best sintering state among the samples examined here, the test of oxygen permeation was carried out. The relationship between the gas evolution rate and the temperature is indicated in Fig. 7. The oxygen concentration in the extracted gas versus temperature relation is also shown in the same figure, where the internal pressure is $6\,cmHg$. The rate becomes obviously greater as the temperature is elevated and, therefore, as the oxide ion conductivity increases. The oxygen concentration of the gas also increases with increasing temperature. We could get the oxygen-enriched gas up to 48% by a one-step operation. The present result indicates that we could not prevent mechanical leakage of air in the

cell. If we could use a perfect apparatus to extract oxygen, 100% pure oxygen would be obtained.

In order to calculate the electrochemical evolution rate of oxygen V_r $(ml\,min^{-1}\,cm^{-2})$, we used the following equation assuming that the mechanically leaking gas has the same composition as that of air,

$$V_r = (X - 0.21\,Y/0.79)V_t/S \tag{6}$$

where X and Y are the oxygen and nitrogen partial pressures in the obtained gas, respectively; $V_t\,(ml\,min^{-1})$ the total gas volume obtained per 1 min; and S (cm^2) the internal sample surface area. On the other hand, the theoretical evolution rate of oxygen V_c $(ml\,min^{-1}\,cm^{-2})$ can be calculated from the current density I $(A\,cm^{-2})$ passed through the sample,

$$V_c = 60IV/4/F/S \tag{7}$$

where F is Faraday constant and V is the molar volume of oxygen. If we assume that the oxygen concentration cell is formed and it is short-circuited by electron holes present in the sample, this equation can be rewritten as follows:

$$V_c = 7.5 \times 10^{-5}(T\sigma_i t_e/L)\ln(0.21 \times 76/H) \tag{8}$$

where $T(K)$ is the cell temperature, $\sigma_i(S\,cm^{-1})$ the ionic conductivity, t_e the electronic transport number, L (cm) the thickness and H (cmHg) the internal pressure of the cell.

Fig. 8 shows the variation of electrochemical evolution rate of pure oxygen against the cell temperature, where the internal pressure was $6\,cmHg$. The broken line indicates the value calculated using equation 8. The practical evolution rates (O) almost correspond to the calculated. Fig. 9 shows the plots of evolution rate against the internal pressure. The observed data also show a good correspondence with the calculated (broken lines) at $1000°C$, but at $800°C$, the value
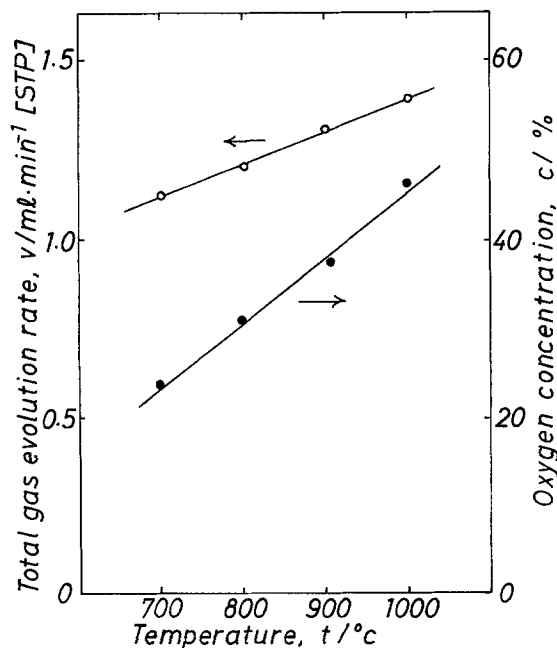

Fig. 7. Gas extraction rate and oxygen concentration versus temperature relationship. Internal pressure: $6\,cmHg$.
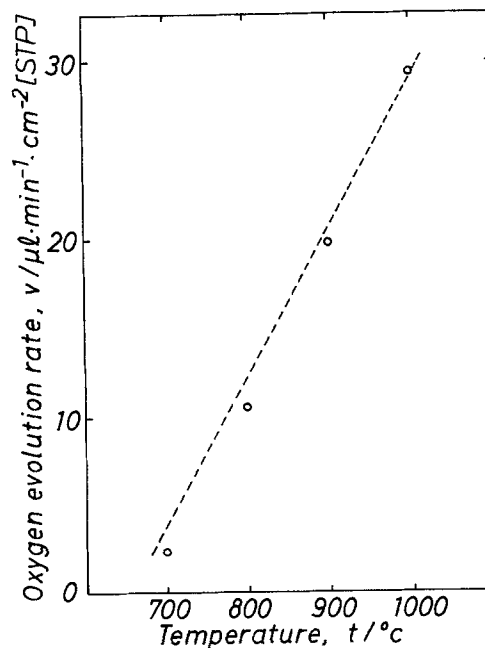

Fig. 8. Electrochemical oxygen evolution rate versus temperature relationship. Internal pressure: $6\,cmHg$.
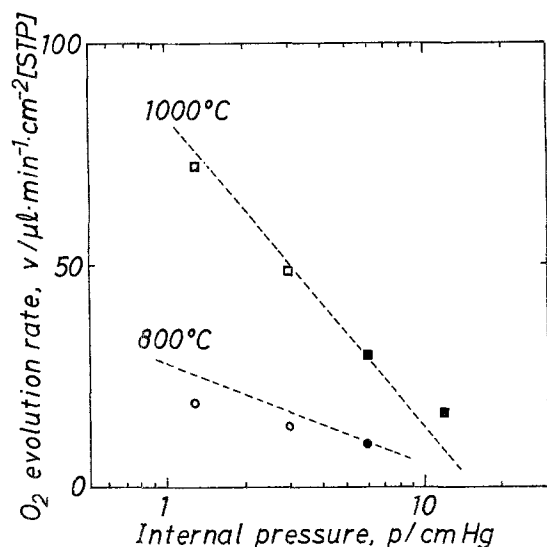
Fig. 9. Electrochemical oxygen evolution rate versus internal pressure relationship. Open and solid symbols mean the data with and without the gas reservoir, respectively.

Fig. 10. Comparison of oxygen extraction using a mixed conductor with that using a silicone film.

decreased especially under low internal pressures. This might be due to the oxygen adsorption on the internal sample surface, which would be same as the polarization behaviour at the anode side of an oxygen concentration cell.

3.5. Comparison of mixed conductor with silicone film as an oxygen separator

The silicone film is now widely used as an oxygen separator film to produce oxygen-enriched air [6]. The silicone film is flexible and can be made in various shapes or forms. However, in contrast to the mixed conductor, pure oxygen gas can not be obtained by one step operation in this method, since the separation is made by the small difference in permeability coefficients between oxygen and nitrogen. Therefore, in order to obtain highly oxygen-enriched gas, we have to repeat the same extraction.

In a silicone polymer film, the gas permeation rate V (ml min^{-1} cm^{-2}) is given by

$$V = P(p_1 - p_2)T/d \qquad (9)$$

where P is the permeability coefficient, p_1, p_2 the partial pressures of gas on both sides of film and d the thickness. The permeability coefficient of oxygen in silicone is about 6×10^{-8} ml cm^{-1} s^{-1} (cmHg)$^{-1}$. For example, in the case of $d = 25\,\mu$m, $p_1 = 16$ cmHg (P_{O_2} in air) and $p_2 = 6$ cmHg, the oxygen gas permeation rate is $14.4\,\mu$l cm^{-2} min^{-1}. However, as nitrogen is also able to permeate the same film ($P = 3 \times 10^{-8}$ ml cm^{-1} sec^{-1} (cmHg)$^{-1}$) in this case, the permeated gas can not be pure oxygen.

On the other hand, if we make the above mentioned mixed conductor a thin film having $25\,\mu$m thickness, we can extract about $1500\,\mu$l cm^{-2} min^{-1} of oxygen at $1000°$ C. Fig. 10 shows the comparison of oxygen evolution rate between the mixed conductor film and the silicone film as a function of P_{O_2}. The circles represent the data for the case of the internal pressure
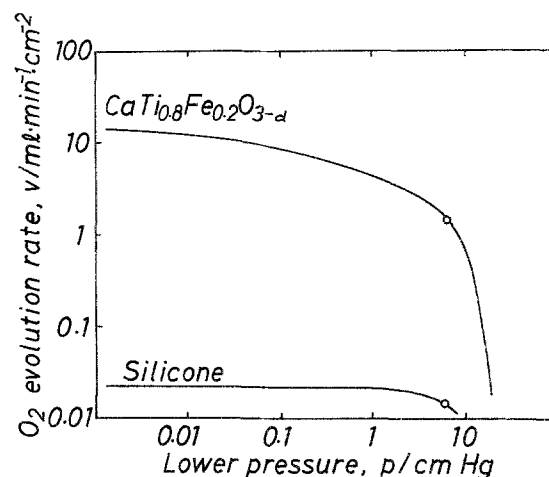
of 6 cmHg mentioned above. It is obvious from this figure that the oxygen evolution rate from the mixed conductor is more than two orders higher than that of the silicone film over a wide range of P_{O_2}. Although the rate in silicone saturates as the P_{O_2} decreases, the rate in the mixed conductor increases monotonically. Furthermore, mixed conductor ceramics are able to be used at high temperature where silicone cannot be employed. If it were possible to make a thin film of the mixed conductor, this method would be potentially useful for oxygen extraction.

4. Conclusion

The substituted oxides of $CaTi_{1-x}Fe_xO_{3-\alpha}$ show two different single crystal phases, a pseudo-cubic for $x = 0.0-0.25$ and a cubic for $x = 0.30-0.50$. In the case of Co- or Ni-substitution, a wide range of solid solution formation range cannot be observed. The Fe-substituted oxides show oxide ion and electron (hole) mixed conduction. The electronic conductivities increase with increasing Fe content. The ionic transport number generally becomes greater with increasing temperature in each composition. In this system, the $x = 0.20$ sample shows relatively high ionic transport number and, also, the highest oxide ion conductivity.

The extraction of oxygen gas from air is possible using an oxide ion and electron mixed conductor such as $CaTi_{0.8}Fe_{0.2}O_{3-\alpha}$ ceramics and a diaphragm pump. The extraction rate of oxygen in this method is higher than that of a conventional silicone film method.

References

[1]   T. Esaka, H. Iwahara and H. Kunieda, *J. Appl. Electrochem.* **12** (1982) 235.

[2]   T. Esaka and H. Iwahara, *J. Appl. Electrochem.* **15** (1985) 447.

[3]   H. Iwahara, T. Esaka and K. Takeda, *J. Amer. Ceram. Soc.* (to be published).

[4]   T. Takahashi, H. Iwahara and T. Ichimura, *Denki Kagaku* **37** (1969) 857.

[5]   T. Takahashi, T. Esaka and H. Iwahara, *J. Solid State Chem.* **16** (1976) 317.

[6]   S. Shimizu, *Energy and Resources* **4** (1983) 178.